TOWARDS 3D REGISTRATION OF FETAL BRAIN MRI AND ULTRASOUND

Maria Kuklisova-Murgasova[1] *Gerardine Quaghebeur*[2] *Joseph V. Hajnal*[3] *J. Alison Noble*[1] *Julia A. Schnabel*[1]

[1] Institute of Biomedical Engineering, Department of Engineering Science, University of Oxford, UK
[2] Neuroradiology, John Radcliffe Hospital, Oxford, U.K.
[3] Imaging Sciences Department, MRC Clinical Sciences Centre, Imperial College London, Hammersmith Hospital, UK

ABSTRACT

We propose a novel method for automatic alignment of fetal brain magnetic resonance image volumes and 3D ultrasound images. Volumetric fetal brain MRI is obtained from reconstructing 2D slices, and is then segmented using a preterm neonatal probabilistic atlas. The segmentation is further refined to extract features that are prominent in fetal brain ultrasound. From the MR segmentation, a pseudo-ultrasound image is simulated, taking into account the direction of the beam in the real ultrasound volume. The simulated and real ultrasound images are then affinely aligned using normalized cross-correlation. We show that the proposed approach performs better than the standard approach for multi-modal registration of the MR and ultrasound volumes driven by normalized mutual information.

Index Terms— Fetal brain imaging, MRI, 3D ultrasound, multi-modal registration

1. INTRODUCTION

Fetal ultrasound (US) is the standard modality for assessing fetal brain development in clinical practice. Though ultrasound can provide relatively high resolution, it is subject to severe artefacts. Traditional methods for assessment of fetal brain development rely on measurements performed on 2D US scans, where a pre-defined plane is manually selected by the radiographer, and several 2D measurements are taken to assess the growth of the fetal head. If a brain abnormality is suspected, fetal MRI is performed to confirm the finding.

Recent advances in developing 3D US probes as well as new methodologies for volumetric reconstruction of fetal brain MRI from thick fast-spin-echo 2D slices provide opportunities for development of new quantitative techniques for assessment of fetal brain development. Recently emerged super-resolution techniques for reconstruction of high-resolution fetal brain MRI allow us to study the brain development in great detail [1]. Detailed models of brain structure constructed from such fetal MR volumes could serve as a prior for quantitative measurements from 3D US.

In this paper we propose a method for 3D alignment of fetal brain MRI to US. This problem has not been explored in literature so far, even though various MR-US and CT-US alignment methods for different organs have been proposed, mainly in the context of computer assisted radiotherapy planning, e.g. [2]. Inspired by [2], we propose to simulate the 3D fetal head US from an MR volume and then align the simulated and real US image volumes. To perform a suitable simulation, we analysed the correspondence of different features present in the fetal head US and MRI volumes, described in Sec. 2. We segmented the chosen structures in one high quality fetal MR volume and created a deformable template of fetal brain, described in Sec. 3. The simulation of US from this template and the alignment is presented in Sec. 4. We evaluate our method in Sec. 5 by performing affine inter-subject registration of the deformable MR template to five US images and show that it outperforms standard multimodal approach in which MR and US volumes are registered directly using normalized mutual information.

This work was supported by the Wellcome/EPSRC Centre of Excellence in Medical Engineering - Personalised Healthcare, WT 088877/Z/09/Z.

2. FEATURES OF FETAL BRAIN US AND MRI

The major challenge in aligning fetal brain MR and US images is that there exists no intensity mapping between the two modalities, as they visualize complementary features. While MRI offers good contrast between soft tissues, especially white matter (WM), grey matter (GM) and cerebro-spinal fluid (CSF), US depicts surfaces of the structures with superior resolution to MRI. The features best detected using US are often hard to detect on MRI, because of its insufficient resolution. Conversely, the WM-GM boundary does not appear in US at all. The main US features which we will use to guide the alignment include [3]

1. the skull
2. the midline (separating the two halves of the brain)
3. the brain surface
4. chloroid plexus (located in the ventricles)
5. septi pelucidi (membranes separating ventricles)
6. cerebellum
7. deep GM

and are shown in Fig.1. The features visible on US are mainly created by the reflection of the acoustic beam at the boundary of structures due to the difference in acoustic impedance (e.g. brain, cerebellum or bone surface, membranes), or the microstructure of the tissue (e.g. in basal ganglia or brain volume). We therefore perform a segmentation of the above structures in one MR image volume, and use this to compute surface gradients to simulate reflection or to add volumetric echogenity to simulate reflection of tissue microstructure. The segmented MR image volume will serve as a deformable template for inter-subject MR-US alignment.

3. DEFORMABLE TEMPLATE OF FETAL BRAIN

3.1. Reconstruction of fetal brain MRI

To obtain a deformable 3D MR fetal brain template, an MR image of a healthy fetus with gestational age (GA) 28 weeks was selected. Fetal brain US often depicts structures that are difficult to visualize

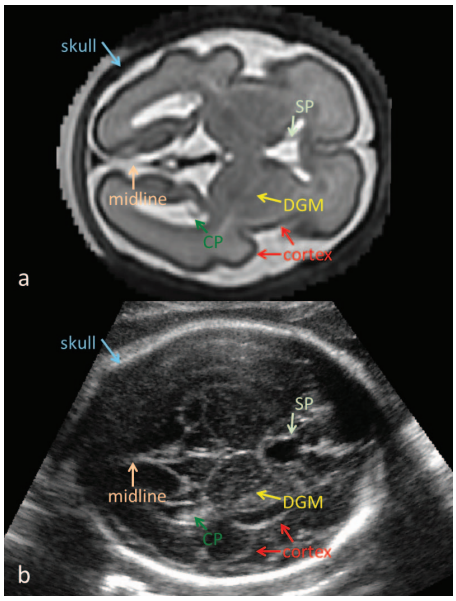


Fig. 1. Features visible on fetal brain US in axial view: skull, cortical surface, midline, DGM, chloroid plexus (CP) and septum pellucidum (SP). Positions of these features in MRI (a) and in US (b).

on MRI (e.g. membranes of the midline), thus a high resolution fetal head MR image is essential for the creation of a deformable template. Six stacks (two in each orthogonal direction) of 2.5mm thick MR image slices with a slice gap 1.25mm and isotropic in-plane resolution of 1.25mm were acquired using single-shot fast spin echo T2w sequence[1]. The volume was reconstructed by iterating between super-resolution reconstruction and slice-to-volume rigid registration using our previously developed fetal MR reconstruction method [4]. The similarity measure used for slice-to-volume registration was normalized mutual information [5]. Our superresolution reconstruction is designed to deal with the common artefacts of MR acquisition, namely exclusion of motion-corrupted slices, intensity matching and bias field correction. The volume was obtained by iterative minimization of the following objective function:

$$\sum_j w_j (y_j^* - y_j^s)^2 \tag{1}$$

where y_j^* denotes voxel intensities of scaled and bias-corrected acquired slices, $y_j^s = \sum_i m_{ij} x_i$ denotes voxel intensities of slices simulated from the latest estimate of the volume with voxel intensities x_i using the point-spread function of MR acquisition sampled into values m_{ij}. The weights w_i are obtained as posteriors of classification of intensity errors between simulated and corrected acquired voxels or slices into outliers and inliers using an EM algorithm (more specifically, w_i is a product of the voxel and slice posteriors). The reconstruction is regularized using edge-preserving smoothing [6]. The reconstructed volume, scaling factors and bias fields are estimated by minimizing the objective function (1) using gradient descent. The combination of this comprehensive and robust reconstruction method together with high sampling and relatively small slice thickness of the acquired dataset results in a high quality fetal head volume suitable for segmentation of the structures visible in fetal US (Fig. 1a and 3a).

[1]We thank the Department of Neonatal Imaging, Imperial College London for providing this dataset.

3.2. Segmentation of the brain in MRI

The reconstructed MRI was upsampled from a resolution with isotropic voxels size 0.75mm to a higher resolution (isotropic voxels with size 0.33mm) and segmented using a preterm neonatal probabilistic atlas [7], publicly available at *www.brain-development.org*. The earliest time-point available at this atlas (29 weeks GA) was chosen. The average T2 template provided with the atlas was aligned with the MR image using multi-resolution B-spline non-rigid registration with final control point spacing 5mm (see [7] for details). The probability maps were then warped to the image space and used as a spatial prior to segment the image into 7 classes (white matter (WM), cortex, deep gray matter (DGM), brainstem, cerebellum, cerebro-spinal fluid (CSF) and background) using EM algoritm [8], by iterating between equations

$$p_{ik} = \frac{P(x_i^*|\mu_k,\sigma_k)p_{ik}^{atlas}}{\sum_k P(x_i^*|\mu_k,\sigma_k)p_{ik}^{atlas}} \tag{2}$$

$$\mu_k = \frac{\sum_i x_i^* p_{ik}}{\sum_i p_{ik}} \tag{3}$$

$$\sigma_k^2 = \frac{\sum_i (x_i^* - \mu_k)^2 p_{ik}}{\sum_i p_{ik}} \tag{4}$$

where x_i^* denotes bias-corrected voxel intensities, p_{ik} the posteriors, and p_{ik}^{atlas} the priors from the probabilistic atlas. $P(x_i^*|\mu_k,\sigma_k)$ are likelihoods modelled by Gaussians with means μ_k and variances σ_k. The exception is the background class, where a mixture of two Gaussians was used to model the likelihood due to the presence of amniotic fluid in background as well as larger proportion of extracranial CSF in fetuses compared to pre-term infants. The bias field was also iteratively corrected during segmentation. The posteriors, means and variances can be used to model the estimate of the bias-free image with voxel intensities $e_i = \sum_k \frac{p_{ik}}{\sigma_k^2}\mu_k / \sum_k \frac{p_{ik}}{\sigma_k^2}$ [8]. The bias field can then be estimated by comparing the image intensities to the estimate followed by weighted Gaussian smoothing [9]. Unlike previous approaches [8, 9], we avoid logarithmic transformation of the intensities in the pre-processing to make the bias field additive, but instead work directly with a multiplicative bias field. At each iteration we calculate the bias residual $r_i = \log(x_i^*/e_i)$. This is followed by weighted Gaussian smoothing of the residual r_i with weights $x_i^* \sum_k \frac{p_{ik}}{\sigma_k}$ to calculate the bias field b_i^n still present at the n^{th} iteration. The bias-corrected image is then updated as follows: $(x_i^*)^{n+1} = (x_i^*)^n \exp(-b_i^n)$.

The automatic segmentation was visually inspected and any minor misclassifications were manually corrected. The CSF segmentation was obtained by joining the bright background tissue and automatic segmentation of CSF. As amniotic fluid is always separated from CSF, the CSF segmentation was obtained by calculating the largest connected component of this joint tissue class.

In fetal brain US, the brain tissue (with exception of the corpus callosum) is clearly divided into a right and left hemisphere. This however is only partially visible on MRI due to insufficient resolution and partial volume effects along the midline. We therefore artificially separated the WM segmentation into two parts (by removing the voxels closer than 1.5mm to the WM surface) and calculated distance transforms from these two WM cores. All the brain structures (except for WM) were thus separated into right or left, depending on their distance to the right or left WM core. Voxels with roughly

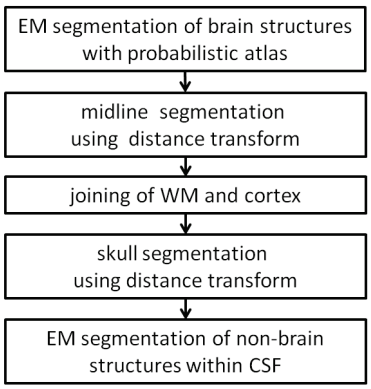


Fig. 2. Overview of the methodology for the segmentation of the deformable MR template.

same distance from both were removed to simulate the presence of a small amount of CSF between right and left part of the brain, visible on US.

Finally, the WM and cortex were joined to create the segmentation of cortical hemispheres, as the WM-cortex boundary is not visible on US.

3.3. Segmentation of the non-brain structures in MRI

Segmentation of skull in MRI is difficult as it appears dark and often borders other tissues also appearing dark on T2w MRI. Additionally, the thickness of the fetal skull is well below 1mm, making it difficult to segment given the resolution of the image. The skull was therefore estimated from the brain mask created by joining automatic segmentations of five brain tissues and CSF, described in Sec. 3.2. A distance transform from this brain mask was calculated, and it was visually determined that the voxels with distance between 0.6mm and 1.4mm delineated the skull very well.

Chloroid plexus, septi pellucidi and membranes of the midline are structures well visible on US. They are located within the CSF and are largely ignored in standard segmentation methods for brain MRI. We therefore segmented the CSF voxels into two classes. The darker class represents the non-brain structures we are interested in. To avoid inclusion of partial volume (PV) voxels where CSF is mixing with neighbouring brain tissue or the skull, we removed all voxels with distance less then 0.75mm from the brain or skull. For classification into dark and bright intensity voxels, we used equations (2), (3) and (4), except that this time we did not use atlas as a prior, but average of the posteriors of the six neighbouring voxels from the previous iterations. The use of the neighbourhood prior, though resulting in slight oversmoothing, ensured a clean segmentation of non-brain structures without inclusion of remaining PV voxels. The final segmentation of the MR deformable template is shown in Fig. 3a. The overview of the segmentation of the MR template is shown in Fig. 2.

4. MR-US ALIGNMENT

For the purpose of alignment of the deformable MR template with 3D US images, we simulated the US image from the segmentation of the MR template, inspired by [2]. The reflections in US are visible when a beam meets a boundary of two tissues with different acoustic impedances. The main surfaces to consider here are the skull surface and the boundary between brain and CSF. In adults, the bone reflects all the signal, thus creating shadows behind the bones. This does not apply to the fetal skull, which is not fully calcified and fused, hence the signal can penetrate through the fontanels and sutures. At present there does not exist a model for acoustic properties of the fetal skull. We therefore assume the beam passes through the skull. This is partly true, as the radiographer tries to find a position of the probe which gives the best view of the fetal brain while minimizing the shadows.

Our simulation of a 3D US image from an MR volume therefore includes reflections of surface of the brain and skull. The brain segmentation is obtained by joining segmentations of cerebral hemispheres, DGM and brainstem. The cerebellum is treated separately, as the cerebellar surface is of too small scale to simulate the reflection. We calculate the gradients $\boldsymbol{g_i}$ of the brain and skull surface which are an estimate of the surface normals. The surface s_i can be estimated as the gradient magnitude $s_i = |\boldsymbol{g_i}|$. Membranes are directly treated as surfaces due to their small thickness. The amount of reflected signal also depends on angle α of the direction of the beam and the surface normal, with highest reflection if their direction is identical. Finally, the amount of signal reflected back to the probe also depends on factors z_i derived from the acoustic impedances of the two tissues [2]. The reflection R_i is therefore calculated as

$$R_i = z_i * cos(\alpha) * s_i \tag{5}$$

Lack of knowledge of tissue properties of the fetal skull and brain prevents us from calculating the amount of signal transmitted through the tissue surfaces. We therefore did not attempt to model attenuation and use the simplified model given by eqn. (5). The values of z_i for skull, brain and membrane surfaces are experimentally determined. Visual inspection of the US also revealed that different tissues have different levels of echogenity. This is highest for chloroid plexus, followed by DGM and brainstem (appearing similar) and cortical hemispheres as darkest. We therefore add visually determined uniform intensity values to these structures. Additionally, the cerebellum is also included as a uniform high-intensity structure. As we do not aim to perform realistic simulation but only include the features which will drive the registration, we do not include speckle in the pseudo-US image. The resulted simulation is presented in Fig. 3b.

The simulated US image is then affinely aligned with the real US image using normalized cross-correlation. The alignment could be done iteratively, as the simulation depends on the direction of the beam. However, the US images are usually acquired in roughly the same position, so only one iteration is used at present.

5. RESULTS

The proposed registration method was applied to five US images of fetal head, with GA 28-29 weeks [2]. Images were acquired using Philips HD9 machine using a 3D transabdominal probe with mechanical steer. Quality of the US fetal brain scans can vary considerably. Only good quality images were selected for experiments, on the criteria of substantial amount of the brain to be visible and attenuation not too high to obstuct visibility of the features. The MR image template was affinely aligned to these images using the proposed method, and for comparison also using normalised mutual information. We found that normalized mutual information was too flexible to find correct correspondences of surfaces which are prominent in these images, and features were often misaligned (see Fig. 3c).

[2]We thank the Intergrowth-21st Consortium for providing the images

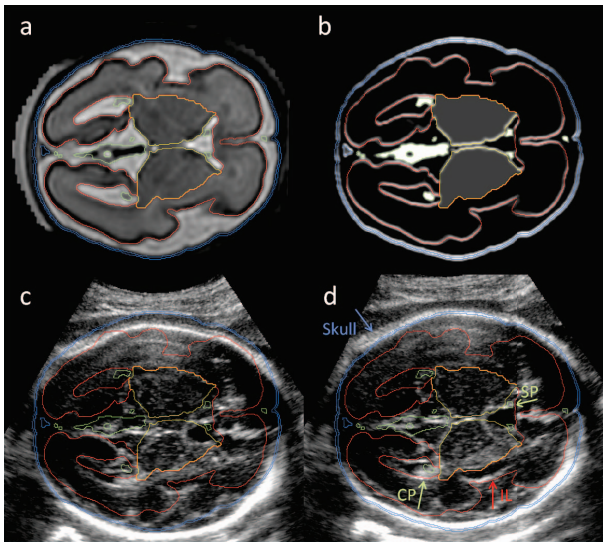


Fig. 3. MR to US alignment. (a) High resolution MR image with the segmentation of skull (blue), brain (red), DGM (yellow) and non-brain structures (green). (b) Simulated US image. (c) Affine alignment using NMI; the features are not well aligned. (d) Affine alignment using the proposed method; the corresponding features are well aligned. Highlighted features: skull, insular lobe of the cortex (IL), chloroid plexus (CP) and septum pellucidum (SP).

Method	No alignment	NMI	Proposed
Scan 1	1.80mm	4.29mm	0.43mm
Scan 2	1.73mm	6.02mm	0.66mm
Scan 3	3.29mm	0.65mm	0.35mm
Scan 4	1.11mm	0.63mm	0.43mm
Scan 5	3.01mm	2.69mm	0.83mm
Average	2.18mm	2.86mm	0.54mm

Table 1. Average distances of midline planes of MR and US volumes after alignment with NMI and proposed method.

Much better results were obtained using the proposed method, as shown in Fig. 3d.

Quantitative evaluation of the quality of alignment of US and MRI is problematic as it is difficult to accurately define 3D landmarks in US images with heavy artifacts and missing features. We therefore investigated distance of the midline of both images. The plane of the midline in MR image was calculated by carefully placing three points. The midline was manually traced in all five US images in two orthogonal directions in regular intervals, wherever visible. We calculated the average distance of these points to the aligned midline plane of the MR image. Results presented in Table 1 show that our proposed method produces good quality alignment of the midline with an average error of 0.54mm, while alignment using NMI is unstable.

6. DISCUSSION AND CONCLUSION

In this paper we proposed a novel method for affine registration of 3D fetal MRI and US. The method was based on simulation of pseudo-US image from a reconstructed MR template. We described a high-resolution reconstruction of fetal brain MRI and atlas-based segmentation of structures in MRI which are the important features visible in fetal brain US. Though the segmentation included a manual correction step, it could be also run automatically with a small drop in the performance, thus enabling 3D registration of any MR and US image of similar GA, for which a probabilistic atlas is available. We demonstarted that our method accurately aligns the midline of the brain in the two modalities, unlike when using registration using NMI. The proposed method will serve as a tool towards better understanding of corresponding features in fetal brain MRI and US. The method performed well when good quality 3D US scans were used. In the future we would like to further develop our registration methodology to be more robust against artefacts in US and to deal with missing features. This would enable us to register also lower quality scans and perform non-rigid alignment. We would also like to develop a framework for more comprehesive validation of the alignment, which could include definition of the corresponding landmarks and regions of interest in MR and US fetal brain MRI.

7. REFERENCES

[1] Vidya Rajagopalan, Julia Scott, Piotr A. Habas, Kio Kim, François Rousseau, Orit A. Glenn, A. James Barkovich, and Colin Studholme, "Spatiotemporal morphometry of adjacent tissue layers with application to the study of sulcal formation," in *MICCAI (2)*, 2011, pp. 476–483.

[2] W. Wein, S. Brunke, A. Khamene, M.R. Callstrom, and N. Navab, "Automatic CT-ultrasound registration for diagnostic imaging and image-guided intervention," *Medical Image Analysis*, vol. 12, pp. 577–585, Oct. 2008.

[3] Ana Monteagudo and Ilan E. Timor-Tritsch, "Normal sonographic development of the central nervous system from the second trimester onwards using 2D, 3D and transvaginal sonography," *Prenatal Diagnosis*, vol. 29, no. 4, pp. 326–339, 2009.

[4] M. Murgasova, G. Quaghebeur, J.V. Hajnal, and J.A. Schnabel, "Unified framework for superresolution reconstruction of 3D fetal brain mr images from 2D slices with intensity correction and outlier rejection," in *MICCAI Workshop on Image Analysis of Human Brain Development (IAHBD)*, 2011.

[5] C. Studholme, D.L.G. Hills, and D.J. Hawkes, "An overlap invariant entropy measure of 3D medical image alignment," *Pattern Recognition*, vol. 32, no. 1, pp. 71–86, 1999.

[6] P. Charbonnier, L. Blanc-Feraud, G. Aubert, and M. Barlaud, "Deterministic edge-preserving regularization in computed imaging," *IEEE Transactions on Image Processing*, vol. 6, no. 2, pp. 298 –311, Feb. 1997.

[7] Maria Kuklisova-Murgasova, Paul Aljabar, Latha Srinivasan, Serena J. Counsell, Valentina Doria, Ahmed Serag, Ioannis S. Gousias, James P. Boardman, Mary A. Rutherford, A. David Edwards, Joseph V. Hajnal, and Daniel Rueckert, "A dynamic 4D probabilistic atlas of the developing brain," *NeuroImage*, vol. 54, no. 4, pp. 2750 – 2763, 2011.

[8] K. Van Leemput, F. Maes, D. Vandermeulen, and P. Suetens, "Automated model-based bias field correction of MR images of the brain," vol. 18, no. 10, pp. 885–896, 1999.

[9] W.M. Wells III, W.E.L. Grimson, R. Kikinis, and F.A. Jolesz, "Adaptive segmentation of MRI data," *IEEE Transactions on Medical Imaging*, vol. 15, no. 4, pp. 429–442, 1996.